Characterization of active-passive Al-containing lasers in the COBRA generic photonic integration platform

F. Lemaître[1,2], J. Decobert[2], H. Ambrosius[1], K. Williams[1]

[1] COBRA Research Institute, Eindhoven University of Technology, P.O box 513 5600 MB, Eindhoven, The Netherlands
[2] III–V Lab, Campus de Polytechnique, 1 avenue Augustin Fresnel, F-91767 Palaiseau Cedex, France

This work presents the characterization of first AlGaInAs quantum wells lasers integrated in the COBRA photonic integration platform. An analysis of the I–V and L–I characteristics of Fabry–Pérot lasers allows a comparative investigation of the material characteristics and the butt-joint quality.

Introduction

In comparison to InGaAsP-quaternary (P–Q) based active layers as used in the COBRA platform, AlGaInAs-quaternary (Al–Q) alloys are known to offer enhanced energy efficiency and operation at elevated temperatures [1], and enable selective area growth (SAG) technique, mastered by the III–V Lab [2], to be combined with the COBRA integration technology [3]. The active-passive integration of the COBRA platform is made through a butt-joint process [4] which is sensitive to surface preparation methods, particularly so when using Al–Q alloys [5]. An active structure using Al–Q in its active layer structure has been implemented with the COBRA generic integration technology. This work presents the measurement of Fabry–Pérot lasers (FP laser) prepared with Al–Q and P–Q active layers, with and without passive waveguides, and with and without butt-joint interfaces to quantify the impact of active-passive integration.

Experiment

Photonic integrated circuits are produced using the same mask set. Two nominally identical Al–Q wafers (1 and 2) have been fabricated in order to observe process related variations, and the P–Q wafer fabrication was previously made in a multi-project wafer run [6]. The Al–Q wafers have been prepared using an active layer stack grown at the III-V Lab [4]. The regrowth and process steps have been performed at TU/e following the COBRA generic process flow to create active-passive integrated circuits [3].
For each Al–Q wafer, the analysis of the influence of butt-joint and waveguides losses on the the FP laser requires three different structures as shown schematically in Figure 1: One active-passive laser with long passive waveguide sections, one active laser with butt-joint interfaces, and one all-active butt-joint-free laser structure. They all have a 750 µm long active section, and differ by the length of their passive sections and the presence or otherwise of the butt-joint interfaces. The initial design has a total cavity length of 4.6 mm, ending with two cleaved facets. In order to dispense with the influence of the passive waveguides but keeping the butt-joint interfaces in the structure, this laser has been cleaved 50 µm outside the active section and measured again. The third structure is

a 750 µm long all-active and butt-joint-free laser which has been cleaved from a longer active device. In this way it is possible to observe the influence of the butt-joint interface and the active section itself on the laser L–I and I–V characteristics.
All facets are as cleaved, providing a 33 % reflection back into the waveguide and transmitting the rest of the light out of the chip. As a control experiment, measurements are additionally performed on a 750 µm long all-active butt-joint-free P–Q laser with the same design.

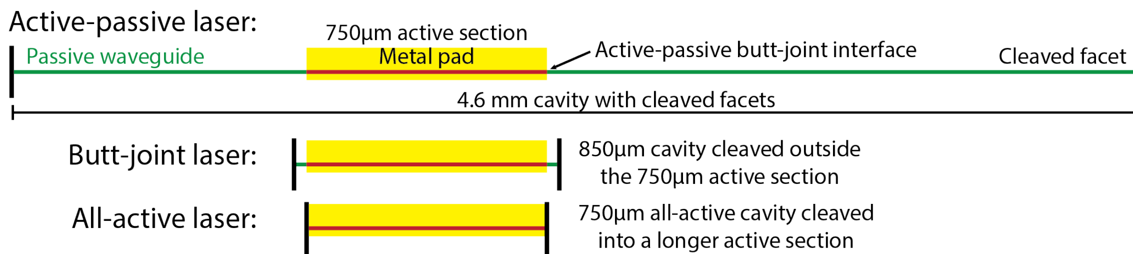

Figure 1: Design of the 3 Fabry–Pérot laser types with 750 µm long active sections.

The laser dies are placed on a gold-plated plate kept at 20 °C using a Peltier module. A large-area photodetector is placed at a distance of 1 mm to record the total output optical power coming out on one side of the chip. The measurement of optical power versus current injection (L–I curve) allows the extraction of the threshold current and the slope efficiency for one output waveguide. The current-voltage (I–V) characteristic of the devices are also measured to investigate leakage paths.

L–I characteristic

The L–I characteristics presented in Figure 2a are obtained by scanning the voltage applied to the device from 0 V to 1.4 V with a 0.05 V step and measuring the current passing through the device up to a maximum of 100 mA. Five lasers have been measured on the same setup in order to compare their threshold current and slope efficiency, summarized in Table 1.

The first Al–Q 4.6 mm long extended cavity laser from wafer 1 did not enter a lasing regime. This device was therefore cleaved to remove the passive waveguides, while retaining the two butt-joint interfaces, leading to a 850 µm long cavity. This re-cleaved structure shows lasing behavior with a threshold current of 47.7 mA. In the case of an all-active and butt-joint-free 750 µm long laser cleaved from a longer active section on the same wafer, a lasing regime with a threshold current of 22.2 mA is reached. This result indicates that the butt-joint interfaces may induce large losses in the device, increasing the threshold and reducing the slope efficiency.

On the second Al–Q wafer, the extended cavity laser shows a threshold current of 25.7 mA and a slope efficiency at threshold of 102 mW/A. After cleaving the laser just outside of the active section, the threshold current is reduced from 25.7mA to 22.8mA and the slope efficiency increases to 124 mW/A. An all-active 750 µm long FP laser from this wafer shows threshold current and slope efficiency of 21.1 mA and 130 mW/A.

These results are consistent with measurements on other devices from the same wafers. Lasers with a butt-joint give poor lasing performance on wafer 1 and a respectable laser performances with wafer 2, and butt-joint-free structures show similar lasing performances.

Wafer	Laser number	Laser type	Cavity length (μm)	Threshold Current (mA)	Slope Efficiency (mW/A)
Al–Q 1	1	Active-passive	4600	–	–
		Butt-joint	850	47.7	66
	2	All-active	750	22.2	139
Al–Q 2	3	Active-passive	4600	25.7	102
		Butt-joint	850	22.8	124
	4	All-active	750	21.1	130
P–Q	5	All-active	750	17.1	143

Table 1: Summary of threshold currents and slope efficiencies of 3 FP laser types for 2 Al–Q wafers and one all-active FP laser from a P–Q wafer.

To further explore the origins of laser behavior, the I-V characteristics of the lasers are measured, as shown in Figure 2b.

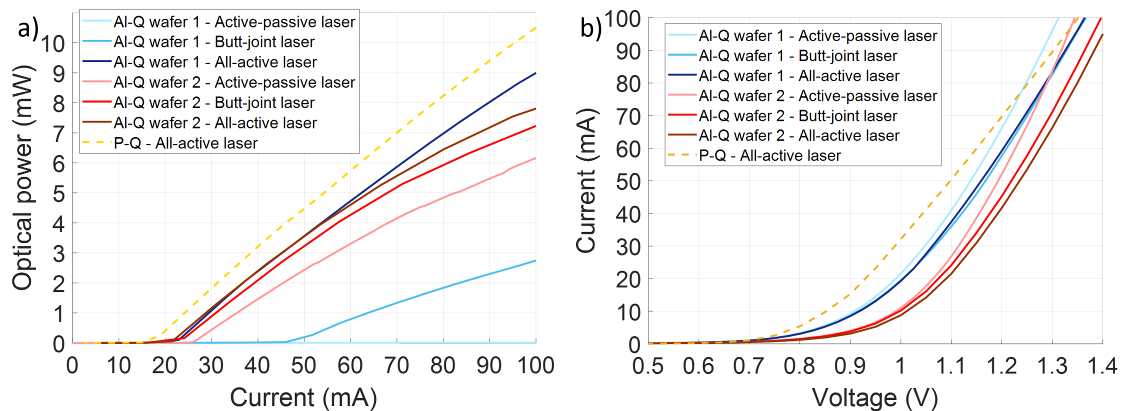

Figure 2: a) L–I characteristic of 3 FP laser types for 2 Al–Q wafers and one all-active FP laser from a P–Q wafer. b) I–V characteristics of the same lasers.

I–V characteristic

The I–V characteristics presented in Figure 2b are obtained by scanning the voltage from 0 V to 1.4 V with a 0.05 V step and measuring the current passing through the device up to a maximum of 100 mA. The result allows the extraction of the turn-on voltage of the structure, and the possible presence of parasitic effects on the diode characteristic.

On both Al–Q wafers, the slope of the I–V characteristic for the active-passive laser is higher than for the butt-joint laser, after cleaving off the passive waveguides, indicating a leakage current via the passive section.

The P–Q laser exhibits a turn-on voltage of 0.8V which is consistent with the operating wavelength. The Al-Q lasers exhibit higher turn-on voltages of 0.9V and 1.0V despite the

same operating wavelengths. There is a difference in turn-on voltage between the two Al-Q wafers, but there is no evident change with and without passive regions and butt-joints. Differences in performance between wafers and with and without butt joints and passive regions may result from both electrical and optical loss mechanisms. This is the subject of ongoing analysis.

Conclusion

Al-Q active layers have been incorporated into the COBRA platform for the first time. Success of integration is evaluated in terms of laser performance with and without passive and butt-joints. Near comparable result is observed for one of two Al-Q wafers, but there is evidence of impaired performance due to the butt-joint integration for the second wafer.

Acknowledgments

The authors would like to thank the European Commission for funding this research through the Marie Curie GeTPICs project (Funded under: FP7-PEOPLE).

References

[1] Wataru Kobayashi, Masakazu Arai, Takayuki Yamanaka, Naoki Fujiwara, Takeshi Fujisawa, Takashi Tadokoro, Ken Tsuzuki, Yasuhiro Kondo, and Fumiyoshi Kano. Design and fabrication of 10-/40-Gb/s, uncooled electroabsorption modulator integrated DFB laser with butt-joint structure. *Journal of Lightwave Technology*, 28(1):164–171, 2010.

[2] J. Decobert, P. Y. Lagrée, H. Guerault, and C. Kazmierski. ”AlGaInAs Selective Area Growth for high-speed EAM-based PIC Sources”. In *Proc. 25th IPRM conference*, pages 16–17, 2013.

[3] M. Smit, X. Leijtens, H. Ambrosius, E. Bente, J. van der Tol, and al. ”An introduction to InP-based generic integration technology”. *Semiconductor Science and Technology*, 29(8):083001, 2014.

[4] F Lemaître, H Ambrosius, J Decobert, M Achouche, P Van Veldhoven, and K Williams. Implementation of the selective area growth in the cobra generic photonic integration platform. In *Proc. 20th Symposium IEEE Photonics Society Benelux*, pages 91–94, 2015.

[5] I. V. Kulkova, S. Kadkhodazadeh, N. Kuznetsova, A. Huck, E. S. Semenova, and K. Yvind. ”High-quality MOVPE butt-joint integration of InP/AlGaInAs/InGaAsP-based all-active optical components”. *Journal of Crystal Growth*, 402:243–248, 2014.

[6] Luc M Augustin, Rui Santos, Erik den Haan, Steven Kleijn, Peter JA Thijs, Sylwester Latkowski, Dan Zhao, Weiming Yao, Jeroen Bolk, Huub Ambrosius, et al. Inp-based generic foundry platform for photonic integrated circuits. *IEEE Journal of Selected Topics in Quantum Electronics*, 24(1):1–10, 2018.